Arch. Metall. Mater. **64** (2019), 1, 371-376

DOI: 10.24425/amm.2019.126262

L. PEREIRA*#, M.R. BELLÉ*, L.F. SEIBEL JÚNIOR*, W.M. PASINI*,
R.F. DO AMARAL*, V. KARLINSKI DE BARCELLOS*

AUSTEMPERING IN ZAMAK BATH: INFLUENCE OF AUSTEMPERING TIME AND AUSTENITIZING TEMPERATURE ON DUCTILE CAST IRON PROPERTIES

The combination of the austempered ductile iron mechanical properties strongly depend on the parameters used on the austempering cycle. On this study, the influence of austempering time and austenitizing temperature on the properties of a ductile iron were evaluated. A metallic bath of Zamak at 380°C was used as an austempering mean. A set of ductile iron blocks were austenitized at 900°C for 90 minutes and submitted to different austempering times in order to determine the best combination of microstructural and mechanical properties. After the definition of the time of austempering, the reduction of the austenitizing temperature was evaluated. The best combination of properties was obtained with austenitizing at 860°C and austempering during 60 minutes.

Keywords: Austempered Ductile Iron, Metallic Bath, Zamak

1. Introduction

Austempered Ductile Iron (ADI) exhibits a good combination of mechanical resistance and tenacity, with elevated wearing resistance. ADI has mechanical properties similar or superior to forged steel, with a fabrication cost by resistance unit much inferior. The material properties are a result of its microstructure, ausferrite which is composed of high carbon austenite, acicular ferrite and also graphite nodes. ADI is a low cost alternative for welded, forged or cast steel and aluminum components, creating opportunities for the cast iron industry [1-2].

ADI properties are related to the production variables and the heat treatment cycle. Regarding the fabrication, the main variable is the alloy composition which may receive Mn and Mo additions to increase hardness and austemperability, and Cu and Ni to increase ductility and also impact resistance. The main heat treatment cycle parameters are the austenitizing temperature ($T\gamma$), austenizing time ($t\gamma$), austempering temperature ($T\alpha$) and austempering time ($t\alpha$) [3-5].

Austenitizing temperature exercises a significantly influence on the tenacity and elongation of ADI, even when submitted to different austempering temperatures [6]. It is expected low austempering temperature, inferior to 350°C, contributes to ADI getting where the hardness and mechanical strength gains are more significant than the gains on ductility and tenacity. On the other hand, when austempering temperatures are applied, superior to 350°C, the trend is to obtain an ADI with greater gains related to tenacity and ductility if compared to mechanical strength [7].

Austempering process is traditionally performed in cast salt bath which is a mix of potassium nitrate, sodium nitrate and sodium nitrite. The great disadvantage of the salt bath is its pollution potential [8-9].

An alternative to this process is metallic bath. Zn-Al and Zn-Sn eutectic alloys were successfully utilized in a laboratorial level [10]. Zamak (Zn-Al-Mg-Cu), according to the previous study, can be used as austempering bath for ADI obtention, at austemper temperatures superior to 375°C [11]. Zn-Al-Cu-Mg alloys possess a heat capacity, in the liquid phase, superior to 0.5 $J(g°C)^{-1}$, where the Mg acts reducing the liquidus temperature [12]. Besides this, the advantages of using Zamak are: its great availability and, after its use as an austempering bath, it is available for recycling process.

The austemper reaction occurs with the nucleation and growth of acicular ferrite (α_{ac}) through grain boundaries or graphite and carbon segregation and diffusion in the austenite phase (γ). The growth of ferrite plates allows the increase of the carbon content on the remaining austenite [13]. This step, demonstrate in Eq. (1), is the first stage of the transformation which, when complete, confers the best properties combination to ADI.

$$1^{o} \text{ stage: } \gamma \rightarrow \alpha_{ac} + \gamma_{HC} \quad (1)$$

$$2^{o} \text{ stage: } \gamma_{HC} \rightarrow Fe_3C + \alpha \quad (2)$$

Elevated content of high carbon austenite (γ_{HC}) is obtained in the end of the first stage, reaching, thus, an increased of thermal and mechanical stability. This stability occurs due to the high carbon content in the austenite solid solution. The time compre-

* FEDERAL UNIVERSITY OF RIO GRANDE DO SUL – SCHOOL OF ENGINEERING – FOUNDRY LABORATORY, PORTO ALEGRE, BRAZIL

Corresponding author: leonardo.pereira@ufrgs.br

hended between the end of the first stage and the beginning of the second stage of the austempering reaction is denominated process window, where the percentage of high carbon austenite is the highest, which results in a toughness increase. As the isothermal austempering treatment follows, carbides precipitation and ferrite (α) formation, from the high carbon austenite, will occur. This is the second stage of the austempering reaction, demonstrate in Eq. (2), which is undesired on ADI, because it leads to toughness and ductility decrease on the material [14-15].

Studies regarding simulations through neural networks and models contribute, significantly, to the process window determination and to the prediction of mechanical properties, yet they possess an error associated to the calculated values [16-17]. The combined effect of the alloy elements and the austempering cycle parameters are qualitatively known, however, by means of mathematical modeling, there is not an efficient method to accurately determine the mechanical properties of a ductile iron submitted to an austempering cycle yet. An experimental evaluation is necessary to determine these properties with accuracy.

In this work, the austempering time and austenitizing temperature for the studied alloy were determined in order to obtain the best combination of microstructural and mechanical properties, using a zamak bath as an austempering mean.

2. Materials and methods

Ductile cast iron with chemical composition as presented in Table 1 was used for this study. Ductile cast iron, of predominantly pearlitic matrix Fig. 6-A, has 150 nodes/mm2 and more than 95% of the nodes are type I and II. The nodules count was performed through the Buehler OmniMet software, with 100× magnification images, obtained from an Olympus BX60M microscope. Nodularity was determined by the comparison method (according to ASTM A247-17 [18]).

TABLE 1

Ductile cast iron chemical composition (% weight)

C	**Si**	**Mn**	**Cu**	**Ni**	**Mo**
3.56	2.30	0.32	0.66	0.53	0.18
Mg	**Sn**	**S**	**P**	**Cr**	**Fe**
0.034	0.02	0.07	0.021	0.03	Balance

Ductile iron was produced in a medium frequency induction furnace, with a charge composed of cast iron return, classified steel scrap, graphite, silicon carbide, ferrosilicon, copper and nickel. Spheroidization treatment occurred by the addition of 1% Fe-45Si-8Mg in a 500 kg ladle by the sandwich method. The ferromolybdenum was added at this stage as well. Inoculation occurred with the addition of 0.6% Fe-Si-La, during the transfer of the molten metal from the spheroidization ladle to the pouring ladle. Then, the metal was poured into green sand molds, at approximately 1420°C. The ductile iron used in the experiment is taken from the as-cast parts in the shape of blocks, with dimensions of 17×17×105 mm and 17×17×65 mm.

To each cycle was employed a three-block set (measuring 17×17×105 mm each block) aimed at the machining of tension specimens, and four block set (measuring 17×17×65 mm each block) aimed at the designing of impact test specimens (Charpy).

The blocks sets were submitted to seven different austempering cycles. In part one only the austempering time was changed. The following parameters were employed on the cycles:

– T_γ = 900°C; t_γ = 90 minutes,
– T_α = 380°C (±5°C); t_α = 15, 30, 60, 90 and 120 minutes.

In part two, only the austenitizing temperature was changed, in order to improve ductility and impact toughness. Austempering time was defined on the basis of the optimized combination of mechanical properties and time obtained in part one. The following parameters were employed on the cycles:

– T_γ = 860 and 820ºC; t_γ = 90 minutes,
– T_α = 380°C (±5°C); t_α = 60 minutes.

As austempering environment, a Zamak alloy was used, the chemical composition is shown at Table 2.

TABLE 2

Zamak alloy chemical composition (% weight)

Al	**Cu**	**Mg**	**Fe**	**Si**	**Zn**
4.25	1.90	0.12	0.30	0.02	Balance

After the heat treatment cycle implementation, the blocks were air-chilled. The thin layer of Zamak that covered the blocks was manually removed. Then the blocks were forwarded to machining operations, in order to manufacture the test specimens and execute the tensile test (according to ASTM E8M [19]) and Charpy impact test (according to ASTM E.23 [20]). In regions without deformation on the test specimens it was performed hardness measurements and microstructure analysis (according to ASTM E3 [21]), 3% nital etching followed by 10% sodium metabisulfite etching was performed in order to contrast martensite. To assist the phase identification from the 15 min and 30 min austempering cycles, 10 microhardness measurements were performed on each specimen, using a Shidmazu microhardness testing machine, applying a load of 100 gf for 15 s.

X-ray diffraction was performed on the specimens exposed to austenitizing temperature of 900°C and 15 min, 60 min and 120 min austempering cycles. The X-ray analysis was conducted on a Philips machine with monochromatic CuKα radiation. The 2θ scan angles varied from 20° to 105°. The current and voltage settings were 40 mA and 40 KV.

3. Results and discussion

The average results of the tensile tests as a function of austempering time are presented in Fig. 1. The austempering time of 120 minutes is the one that contributes most significantly to the increase of ultimate tensile strength (UTS), yield strength

(YS) and elongation (e). On the other hand, austempering time of 120 minutes lead to an impact toughness decrease, if compared to austempering times of 60 and 90 minutes.

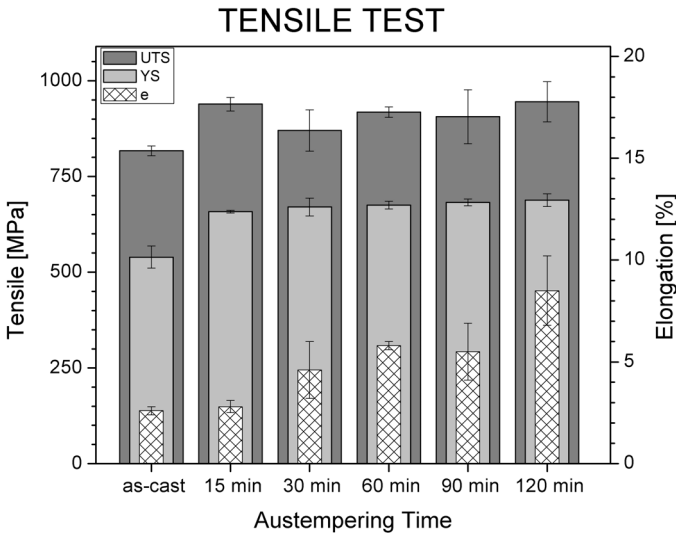

Fig. 1. Mechanical properties for as-cast and austempered ductile iron as a function of austempering time. Ultimate Tensile Strength (UTS), Yield Strength (YS) and Elongation in 36 mm (e)

In the impact test it was observed an impact toughness reduction at 15 and 30 minutes, as it is shown in Fig. 2. A significantly increase in hardness at 15 minutes has also occurred. On the austempering times of 60 and 90 minutes, the mechanical properties are similar, specially observing the standard deviation. The microstructure does not show coarse regions, as it can be seen in Fig. 6 (D and E).

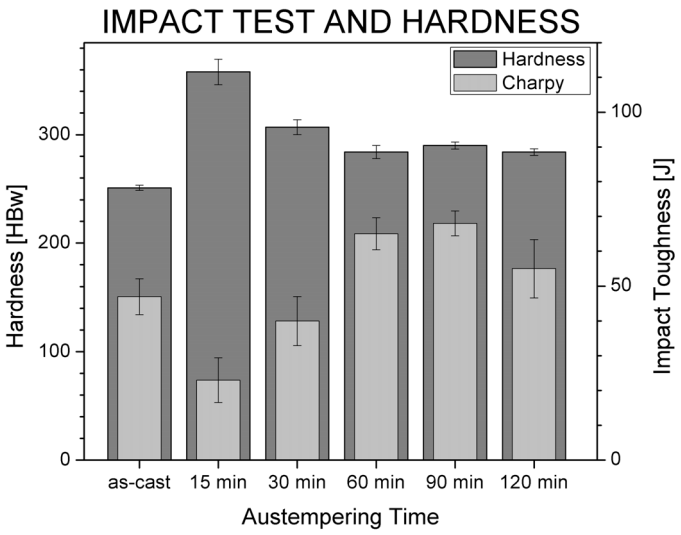

Fig. 2. Brinell hardness and unnotched Charpy test results as a function of austempering time. The values are an average of the highest three test values of the four tested samples

Acicular ferrite growth and carbon diffusion to remaining austenite are phenomenons that require time. Short austempering times are not enough to turn austenite thermal and mechanically stable, so that the material, when requested or chilled, leads to martensite formation, causing impact toughness reduction and hardness increase. This explains the results obtained from the cycles of 15 and 30 minutes, specially when observing the microstructure in Fig. 6 (B and C).

The average results of the tensile tests as a function of austenitizing temperature are presented in Fig. 3.

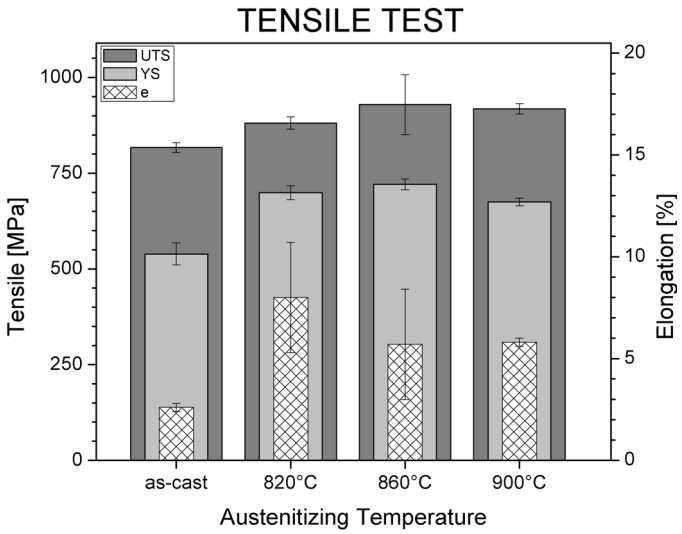

Fig. 3. Mechanical properties for as-cast and austempered ductile iron as a function of austenitizing temperature. Ultimate Tensile Strength (UTS), Yield Strength (YS) and Elongation in 36mm (e)

At 860°C austenitizing temperature, it was observed a greater increase on impact toughness, as shown in Fig. 4. Significant variations on hardness, in function of austenitizing temperature, were not observed.

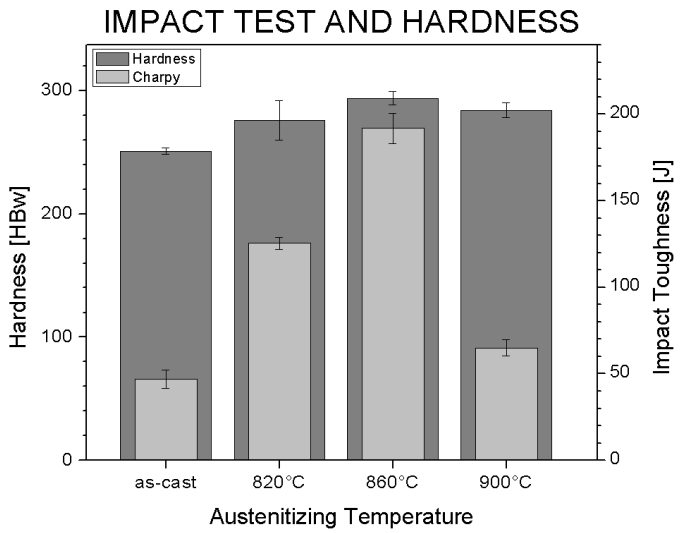

Fig. 4. Brinell hardness and unnotched Charpy test results as a function of austenitizing temperature. The values are an average of the highest three test values of the four tested samples

The microstructural analysis of test specimens from the different cycles enabled the verification of ausferrite forma-

tion. It was observed martensite (α') formation in significant regions of the material from the 15 and 30-min cycles Fig. 6 (B and C).

Studies involving ductile iron alloyed with Cu-Ni-Mo and austempered at elevated temperatures indicate martensite formation in short austempering times, reaching 60% or above in 5 minutes and values close to zero within 1 hour [15, 22-23]. Martensite phase, identified in optical microscopy, is inferred by the microhardness test, in which regions identified as martensite have a measured value of 659 HV (σ = 33 HV). In Fig. 5 it is possible to observe the microhardness difference between both regions. The regions where the transformation presented in Eq. 1 occurred have an average microhardness value of 410 HV (σ = 34 HV), for the austempering cycles of 15 and 30 minutes.

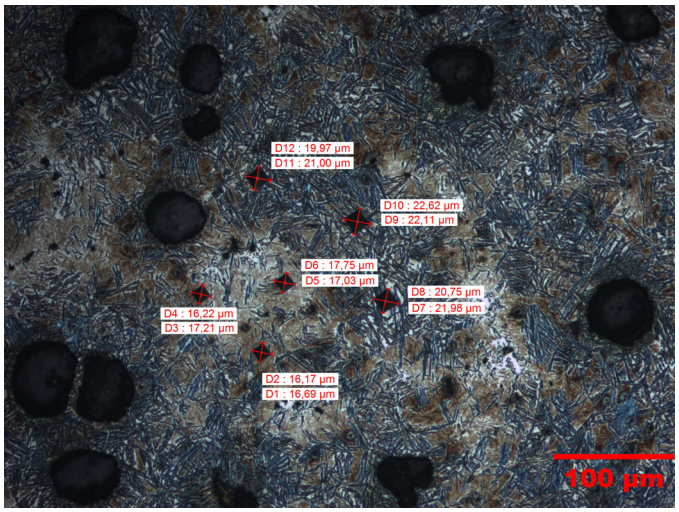

Fig. 5. Microhardness measurements of a specimen austempered for 15min. The color brown corresponds to martensite phase

After 60 min of austempering, as shown in Fig. 6 relevant microstructural modification is not observed in optical microscopy. This is in accordance with Perez, Cisnero and Lopez observations, in 2006, on a ductile iron alloyed with Cu-Ni-Mo and austempered at 370°C. In this case, the maximum content of high carbon austenite was measured at 60 minutes of austempering treatment, slight reduction on this content at 90 and 120 minutes and significant reduction on the high carbon austenite at 240 minutes of austempering treatment [23].

In the beginning of the austempering process, austenite fraction is equal to 1, however, observing the diffraction diagrams of 15 min austempering cycle, Fig. 7, it is possible to identify that the austenite peak (111) close to 43° is proportionally inferior if compared to the 60 min and 120 min cycles. In addition, also for 15 min cycle, it is possible to observe the enlargement of the peaks close to 43° and 45°, respectively of austenite (111) and ferrite (110). The cause of this effect is the presence of martensite, which superior intensity peaks (101) and (110) correspond to 43.8° and 44.8°, respectively (Ref. Code 00-044-1292).

4. Conclusion

1. On the evaluated alloy, austempering times of 15 and 30 minutes were inadequate, occurring impact toughness reduction of 52% and 15%, respectively.
2. Austempering time of 60 minutes combined with the austenitizing temperature of 860°C, if compared to the as-cast specimens, resulted in the increase of:
   – 308% on the impact toughness and 17% on hardness;
   – 14% on ultimate tensile strength, 34% on yield strength and 120% on elongation.
3. Zamak demonstrated to be a satisfactory austempering mean, presenting sufficient cooling severity in order to avoid pearlite formation on the alloy, being possible its alternative utilization, in relation to salts baths, for austempering treatments with temperatures superior to 375°C.

Acknowledgment

The authors acknowledge financial support provided by CNPq and CAPES (Brazilian Funding Agencies).

REFERENCES

[1] J.R. Keough, K.L. Hayrynen, Automotive Applications of Austempered Ductile Iron (ADI): A Critical Review. SAE Transactions **109**, 344-354 (2000). JSTOR, www.jstor.org/stable/44643847.

[2] J.R. Keough, K.L. Hayrynen, G.L. Pioszak, Designing with austempered ductile iron (ADI). AFS proceedings, (2010).

[3] A. Trudel, M. Gagne, Effect of composition and heat treatment parameters on the characteristics of austempered ductile irons. Canadian Metallurgical Quarterly **36**, 5,. 289-298 (1997). DOI: https://doi.org/10.1179/cmq.1997.36.5.289.

[4] P. Sellamuthu, D.G. Harris Samuel, D. Dinakaran, V.P. Premkumar, Z. Li, S. Seetharaman, Effect of nickel content and austempering temperature on microstructure and mechanical properties of austempered ductile iron (ADI), IOP Conf. Ser. Mater. Sci. Eng. **383**, 1 (2018). DOI: https://doi.org/10.1088/1757-899X/383/1/012069.

[5] Amir Sadighzadeh Benam, Effect of alloying elements on austempered ductile iron (ADI) properties and its process. China Foundry **12**, 1, 54-70 (2015).

[6] M. Bahmani, R. Elliott, N. Varahram, The austempering kinetics and mechanical properties of an austempered Cu-Ni-Mo-Mn alloyed ductile iron. Journal of Materials Science **32**, 4783-4791 (1997). DOI: https://doi.org/10.1023/A:1018687115732.

[7] M. Cakir, Cemal, et al., The effects of austempering temperature and time onto the machinability of austempered ductile iron. Materials Science and Engineering **407**, 147-153 (2005). DOI: https://doi.org/10.1016/j.msea.2005.07.005.

[8] Handbook, A.S.M., Volume **4**: Heat Treating. ASM International 10 (1991).

[9] Ch. Yang, et al., NOx emissions and the component changes of ternary molten nitrate salts in thermal energy storage process. Ap-

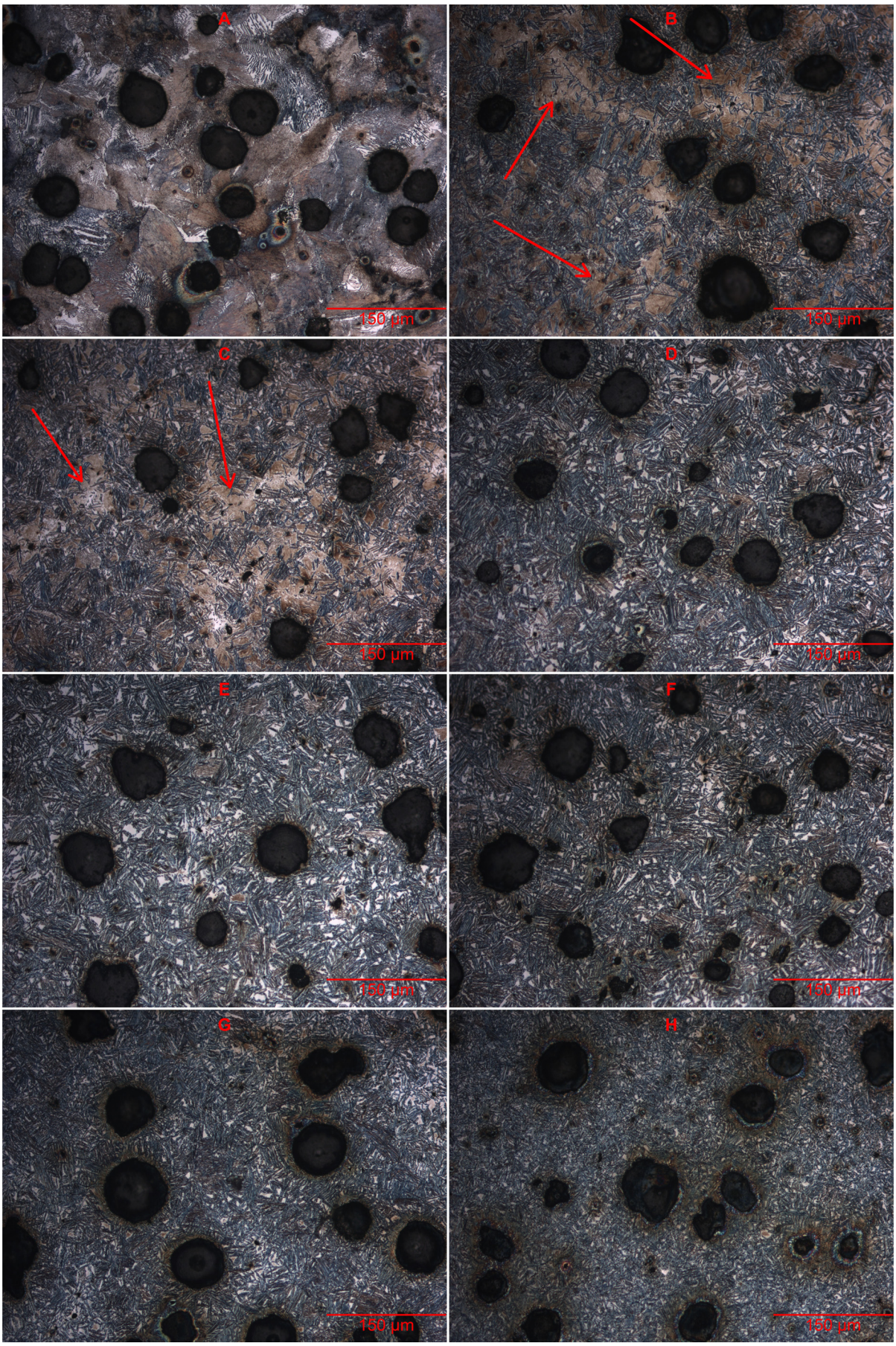

Fig. 6. As-cast ductile iron microstructure with predominantly perlitic structure (A). Microstructure of austenitized at 900°C ADIs austempered for 15 min (B), 30 min (C), 60 min (D), 90 min (E) and 120 min (F). The arrows on figures (B) and (C) indicate the locations where martensite formation occurred. Microstructure of 60 min austempered ADIs austenitized at 860°C (G) and 820°C (H)

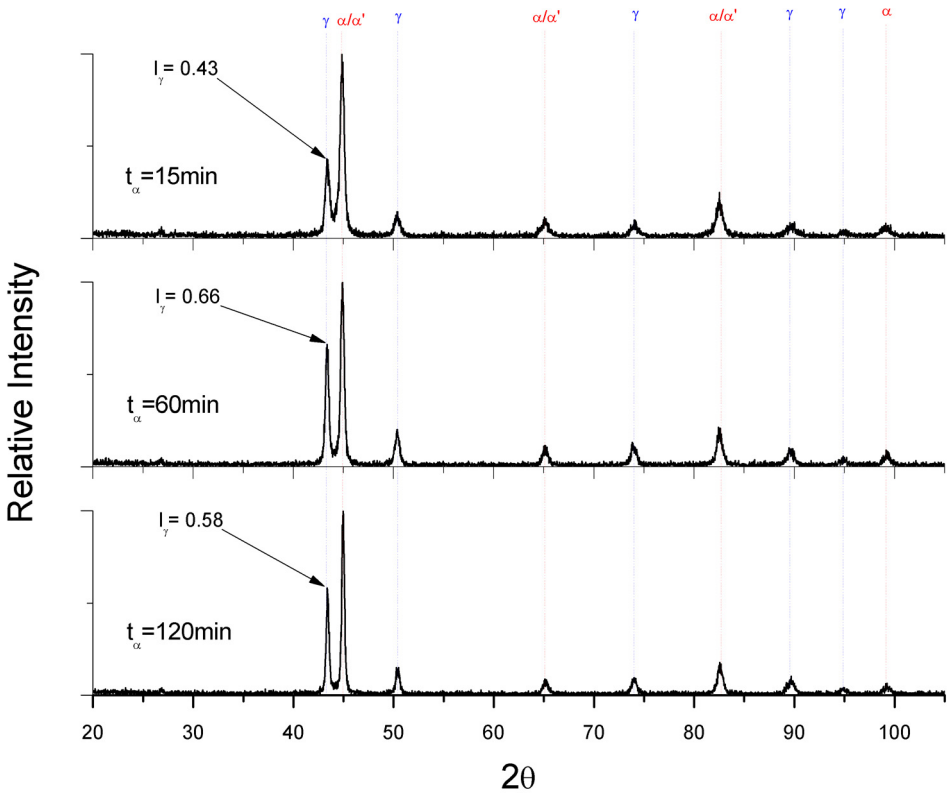

Fig. 7. X-ray diffraction diagrams for ADIs austempered for 15, 60 and 120 minutes

plied energy **184**, 346-352, (2016). DOI: https://doi.org/10.1016/j.apenergy.2016.10.024.

[10] Bruno Vaz de Souza, et al., Austempering heat treatments of ductile iron using molten metal baths. Materials and Manufacturing Processes **33**,15,1667-1673, (2018). DOI: https://doi.org/10.1080/10426914.2018.1424909.

[11] L. Pereira, L.F.S. Júnior, W.M. Pasini, R.F. do Amaral, V.K. de Barcellos, Obtainment of ADI by austempering treatment using zamak 5 bath, Anais do Congresso Anual da ABM, 757-764, (2017). DOI: https://doi.org/10.5151/1516-392X-30312.

[12] M. Krupiński, K. Labisz, T. Tański, B. Krupińska, M. Król, M. Polok-Rubiniec, Influence of Mg addition on crystallisation kinetics and structure of the Zn-Al-Cu alloy. Arch. Metall. Mater. **61,** 2, 785-790 (2016). DOI: https://doi.org/10.1515/amm-2016-0132.

[13] M. Soliman, H. Palkowski, A. Nofal, Multiphase Ausformed Austempered Ductile Iron. Archives of Metallurgy and Materials **62**,3,1493-1498 (2017). DOI: https://doi.org/10.1515/amm-2017-0231.

[14] L. Meier, et al. ,In-situ measurement of phase transformation kinetics in austempered ductile iron. Materials Characterization **85**, 124-133 (2013). DOI: https://doi.org/10.1016/j.matchar.2013.09.005.

[15] M. Górny, E. Tyrała, H. Lopez, Effect of copper and nickel on the transformation kinetics of austempered ductile iron. Journal of Materials Engineering and Performance **23**,10, 3505-351 (2014). DOI: https://doi.org/10.1007/s11665-014-1167-5.

[16] M. Yescas, H.K.D. Bhadeshia, D. MacKay, Estimation of the amount of retained austenite in austempered ductile irons using neural networks. Mater. Sci. Eng. A **311**, 1–2, 162–173 (2001). DOI: https://doi.org/10.1016/S0921-5093(01)00913-3.

[17] R.C. Thomson, J.S. James, D.C. Putman Modelling microstructural evolution and mechanical properties of austempered ductile iron, Materials Science and Technology **16**, 11-12, 1412-1419 (2000). DOI: 10.1179/026708300101507370.

[18] ASTM A247-17 Standard Test Method for Evaluating the Microstructure of Graphite in Iron Castings, ASTM International, West Conshohocken, PA, 2017, https://doi.org/10.1520/A0247-17.

[19] ASTM International. (2016). ASTM E8/E8M-16a Standard Test Methods for Tension Testing of Metallic Materials. Retrieved from https://doi-org.ez45.periodicos.capes.gov.br/10.1520/E0008_E0008M-16A.

[20] ASTM International. (2016). ASTM E23-16b Standard Test Methods for Notched Bar Impact Testing of Metallic Materials. Retrieved from https://doi-org.ez45.periodicos.capes.gov.br/10.1520/E0023-16B.

[21] ASTM E3-11(2017) Standard Guide for Preparation of Metallographic Specimens, ASTM International, West Conshohocken, PA, 2017, https://doi-org.ez45.periodicos.capes.gov.br/10.1520/E0003-11R17.

[22] B. Bosnjak, B. Radulovic, K. Pop-Tonev, V. Asanovic, Microstructural and Mechanical Characteristics of Low Alloyed Ni-Mo-Cu Austempered Ductile Iron. ISIJ Int. **40**, 12, 1246-1252 (2000). DOI: 10.2355/isijinternational.40.1246.

[23] M.J. Pérez, M.M. Cisneros, H.F. López, Wear resistance of Cu-Ni-Mo austempered ductile iron. Wear **260**, 7-8, 879-885 (2006). DOI: 10.1016/J.WEAR.2005.04.001.